Kinetics of spin coherence of electrons in an undoped semiconductor quantum well

M. W. Wu* and H. Metiu
Chemistry Department, University of California, Santa Barbara, California 93106
(Received 16 August 1999; revised manuscript received 24 September 1999)

We study the kinetics of spin coherence of optically excited electrons in an undoped insulating $ZnSe/Zn_{1-x}Cd_xSe$ quantum well under moderate magnetic fields in the Voigt configuration. After clarifying the optical coherence and the spin coherence, we build the kinetic Bloch equations and calculate dephasing and relaxation kinetics of laser pulse-excited plasma due to statically screened Coulomb scattering and electron-hole spin exchange. We find that the Coulomb scattering cannot cause the spin dephasing, and that the electron-hole spin exchange is the main mechanism of the spin decoherence. Moreover the beat frequency in the Faraday rotation angle is determined mainly by the Zeeman splitting, redshifted by the Coulomb scattering and the electron-hole spin exchange. Our numerical results are in agreement with experimental findings. A possible scenario for the contribution of electron-hole spin exchange to the spin dephasing of the *n*-doped material is also proposed.

I. INTRODUCTION

Studies of ultrafast nonlinear optical spectroscopy in semiconductors have attracted numerous interest both experimentally and theoretically during the past 20 years.[1–3] Most of these studies are focused on the optical coherence and the studies of spin coherence are relatively rare. Recently, ultrafast nonlinear optical experiments[4–13] have shown that the spin coherence, which is optically excited by laser pulse, can last much longer than optical coherence. For undoped ZnSe/ZnCdSe quantum wells, it is found in the experiment that the spin coherence can last up to 15-20 ps (Ref. 11) where as for undoped bulk GaAs, it lasts about 600 ps.[13] For *n*-doped materials, the spin coherence can last up to three orders of magnitude longer than in the undoped sample, which makes 8 ns for ZnSe/ZnCdSe quantum well[11] and 100 ns for bulk GaAs.[13] These discoveries have given rise to an emerging interest within the physics and electronic engineering communities in using electronic spins for the storage of coherence and also have stimulated the optimism that the coherent electrons will finally be realized as a basis for quantum computation.

The electron spin coherence can be directly observed by femtosecond time-resolved Faraday rotation (FR) in the Voigt configuration. In that configuration, a moderate magnetic field is applied normal to the growth axis of the sample. The coherence is introduced by a circularly polarized pump pulse that creates electrons and holes with an initial spin orientation normal to the magnetic field. Then the magnetic field causes the electron spin to flip back and forth along the growth axis, which makes the net spin precess about the magnetic field. The hole spin is kept along the growth axis direction of the quantum well as will be discussed below. After a certain delay time τ, a linearly polarized probe pulse is sent into the sample along a slightly different direction from the pump pulse and by measuring the FR angle, one can sensitively detect the net spin of electrons associated with the delay time τ. This method has proven to be extremely successful in measuring the coherent spin evolution and spin dephasing.[4,5,11–13]

In order to further extend the spin coherence time, it is important to understand the physics of spin dephasing. While there is extensive theoretical study and understanding of the optical dephasing,[14] the theoretical investigation on the spin dephasing is relatively limited, nevertheless of much longer history.[15] The early work includes that of Elliott in 1954, who discussed the spin relaxation[16] induced by lattice and impurity scatterings by taking into account the spin-orbit effects.[17] Later, in 1975 Bir *et al.* calculated the spin dephasing using a model Hamiltonian describing the electron-hole spin exchange (EHSE) by considering Coulomb scattering between electron and hole, combined with the spin-orbit-coupling-induced band mixing.[18] In that paper by using Fermi Golden rule, Bir *et al.* proposed a spin relaxation rate that is proportional to the hole density. It was not until the 90s that experimentalists found such an effect and claimed the EHSE is important in the intrinsic and *p*-doped semiconductors.[4,5] For *n*-doped samples, however, as the density of the electrons is much higher than that of the holes, the holes recombine with electrons in a time much shorter than the measured spin dephasing time. As the predicted spin dephasing rate induced by EHSE is proportional to hole density,[18] it is therefore suggested that for *n*-doped sample, the dephasing mechanism is unclear.[11] Recently, Linder and Sham[19] presented a theory of the spin coherence of excitons by studying Bloch equations. However, they did not discuss the dephasing mechanisms explicitly, and instead described all the dephasing by using phenomenological relaxation times.

In this paper, we present a model to study the kinetics of spin precession of a femtosecond laser-pulse-excited dense plasma in a quantum well in the framework of the semiconductor Bloch equations combined with carrier-carrier scattering in the Markovian limit. Non-Markovian effects are not important in our case, as the width of the laser pulse is large (100 fs) and the time scale of spin dephasing is very long. The main purpose of this paper is to understand the spin

decoherence. It has been well known that both carrier-carrier Coulomb scattering and carrier-phonon scattering play significant roles in the optical dephasing. For the two-dimensional (2D) carrier density around 10^{11} cm^{-2} in the experiment,[11] the main carriers are electron-hole plasma and the Coulomb scattering gives a fast dephasing of the optical coherence with dephasing times ranging from tens of femtoseconds to subpicoseconds,[2] depending on the strength and width of the pump pulse and/or the density of doping, which affects the building up of the screening.[14,20] Besides the fast dephasing due to Coulomb scattering, carrier-phonon scattering also contributes to the optical dephasing with the dephasing time being around ten picoseconds and carrier-density independent. For spin coherence, the experimental evidence that the spin dephasing depends strongly on the carrier density[11,13] clearly rules out the possibility that the main mechanism of the spin dephasing is due to carrier-phonon scattering. Therefore, we focus on the effect of carrier-carrier scattering. We distinguish the spin coherence from the optical coherence and study the roles of Coulomb scattering and EHSE to the spin dephasing separately. We find that the pure Coulomb scattering—although it destroys the optical coherence strongly—does not contribute to the spin dephasing at all, and that EHSE is the main mechanism of the spin decoherence.

Our paper is organized as follows: we present our model and kinetic equations in Sec. II. Then in Sec. III we present the numerical results for an undoped $ZnSe/Zn_{1-x}Cd_xSe$ quantum well. A conclusion of our main results and a discussion of the theory for the *n*-doped sample are given in Sec. IV.

II. MODEL AND KINETIC EQUATIONS

A. Model and Hamiltonian

We start our investigation of a quantum well with its growth axis in the *z* direction. A moderate magnetic field *B* is applied in the *x* direction. Landau quantization is unimportant for the magnetic field *B* in our investigation. We consider the conduction band (CB) and the heavy hole (hh) valence band (VB). Due to the presence of the magnetic field, the spins of electrons and holes are no longer degenerate and therefore each band is further separated into two spin bands with spin $\pm 1/2$ for electrons in the CB and $\pm 3/2$ for those in the hh VB. It is noted that these spin eigenstates are defined with respect to the *z* direction.

In the presence of the moderate magnetic field and with the interactions with a coherent classical light field, the Hamiltonian for electrons in the CB and VB is given by

$$H=\sum_{\mu k\sigma}\varepsilon_{\mu k}c^{\dagger}_{\mu k\sigma}c_{\mu k\sigma}+g\mu_B\mathbf{B}\cdot\sum_{\substack{\mu k\\ \sigma\sigma'}}\mathbf{S}_{\mu\sigma\sigma'}c^{\dagger}_{\mu k\sigma}c_{\mu k\sigma'}+H_E+H_I, \tag{1}$$

with $\mu=c$ and v standing for the CB and the VB, respectively. $\varepsilon_{\nu k}$ is the energy spectrum of an electron in the VB (CB) with momentum *k*. It is noted that *k* here stands for a momentum vector in the *x*-*y* plane. $\varepsilon_{\nu k}=-E_g/2-k^2/2m_h\equiv -E_g/2-\varepsilon_{hk}$ and $\varepsilon_{ck}=E_g/2+k^2/2m_e\equiv E_g/2+\varepsilon_{ek}$ with m_h and m_e denoting effective masses of hh and electron separately. E_g is unrenormalized band gap and σ is the spin index. For electron in the CB, $\sigma=\pm 1/2$ and for electron in the hh VB, $\sigma=\pm 3/2$. μ_B is Bohr magneton. $\mathbf{S}_\mu$ are the spin matrices with $\mathbf{S}_c$ being spin 1/2 matrices for electrons and $\mathbf{S}_v$ being spin 3/2 matrices for holes.

H_E in Eq. (1) denotes the dipole coupling with the light field $E_\sigma(t)$ with $\sigma=\pm$ representing the circular-polarized light. Due to the selection rule the electrons in the spin 3/2 $(-3/2)$ hh band can only absorb a left (right) circular-polarized photon and go to the spin 1/2 $(-1/2)$ CB. Therefore,

$$H_E=-d\sum_k\left[E_-(t)c^{\dagger}_{ck(1/2)}c_{\nu k(3/2)}+\text{H.c.}\right]-d\sum_k\left[E_+(t)c^{\dagger}_{ck-1/2}c_{\nu k-3/2}+\text{H.c.}\right]. \tag{2}$$

In this equation, *d* denotes the optical-dipole matrix element. The light field is further split into $E_\sigma(t)=E^0_\sigma(t)\cos(\omega t)$ with ω being the central frequency of the coherent light pulse. $E^0_\sigma(t)$ describes a Gaussian pulse $E^0_\sigma e^{-t^2/\delta t^2}$ with δt denoting the pulse width.

H_I is the interaction Hamiltonian. As said before, we focus on the carrier-carrier scattering. Therefore, H_I is composed of Coulomb scattering and EHSE (Ref. 21) with the latter being much weaker than the Coulomb scattering.[22]

$$H_I=\frac{1}{2}\sum_{\substack{\mu\nu\\ kk'q\\ \sigma\sigma'}}V_q c^{\dagger}_{\mu k+q\sigma}c^{\dagger}_{\nu k'-q\sigma'}c_{\nu k'\sigma'}c_{\mu k\sigma}+\frac{1}{2}\sum_{\substack{\mu\neq\nu\\ kk'q\\ \sigma\sigma'}}U_q\sigma\sigma' c^{\dagger}_{\mu k+q\sigma}c^{\dagger}_{\nu k'-q\sigma'}c_{\nu k'\sigma'}c_{\mu k\sigma}+\frac{1}{2}\sum_{\substack{\mu\neq\nu\\ kk'q\\ \sigma\sigma'}}U'_q\sigma\sigma' c^{\dagger}_{\mu k+q\sigma}c^{\dagger}_{\nu k'-q\sigma'}c_{\mu k'\sigma}c_{\nu k\sigma'}. \tag{3}$$

The first term of Eq. (3) is the ordinary Coulomb interaction. The second term describes the ''direct'' EHSE, which scatters an electron in the band μ with spin σ and momentum *k* to the same band with spin σ and momentum $k+q$ and in the mean time, which scatters an electron from the different band ν $(\neq\mu)$ with spin σ' and momentum k' back to that band with spin σ' and momentum $k'-q$. The last term is ''exchange'' EHSE which scatters an electron in the band μ with spin σ and momentum k' to the different band ν $(\neq\mu)$ with spin σ' and momentum $k'-q$ and in the mean time, which scatters an electron from the band ν with spin σ' and momentum *k* back to band μ with spin σ and momentum $k+q$. It is noted here that σ and σ' stand for $\pm 1/2$ when they are at the CB and $\pm 3/2$ when they are at the VB. As the exchange effect involves a form factor that consists the overlap of the wavefunctions of the CB and VB, U'_q is much smaller than U_q. Moreover, it will be shown later that the

exchange effect is also energetically unfavorable as it scatters carriers across the band. Therefore, the direct EHSE is the dominant effect.

For the Voigt configuration, as **B** is along the x direction and $(S_v^x)_{\pm 3/2,\pm 3/2} \equiv 0$, one can see directly from Eq. (1) that the spin of hh cannot be flipped by the magnetic field. We point here that this is only true when the magnetic field is small compared to the hh light-hole splitting and hence the flip between the hh and the light hole can be neglected in the timescale of the discussion. As $\mathbf{S}_c^x = \sigma^x/2$ with σ^x standing for Pauli matrix, it is therefore straightforward to see from the Hamiltonian that the magnetic field causes the CB electron spin to flip and flop.

It can be seen directly from the Hamiltonian H_E that the laser pulse introduces the optical coherences into the system, which are built between the CB and the VB with same spin direction: $p_{k(1/2)(3/2)} \equiv \langle c^\dagger_{vk(3/2)} c_{ck(1/2)} \rangle$ and $p_{k(-1/2)(-3/2)} \equiv \langle c^\dagger_{vk(-3/2)} c_{ck(-1/2)} \rangle$. In the mean time, due to the presence of the magnetic field in Eq. (1), these optical coherences may further transfer coherence to $p_{k(-1/2)(3/2)} \equiv \langle c^\dagger_{vk(3/2)} c_{ck(-1/2)} \rangle$, $p_{k(1/2)(-3/2)} \equiv \langle c^\dagger_{vk(-3/2)} c_{ck(1/2)} \rangle$, and $\rho_{cck(1/2)(-1/2)} \equiv \langle c^\dagger_{ck(-1/2)} c_{ck(1/2)} \rangle$, with the first two being the coherence between the CB and VB with opposite spin directions and the last one being the coherence between two CB's with opposite spin directions. While it is well known that optical coherence is represented by $p_{k(1/2)(3/2)}$ and $p_{k(-1/2)(-3/2)}$, we will show later that the spin coherence of electrons is represented by $\rho_{cck(1/2)(-1/2)}$. When there is no dephasing effect added on this term, the electron spin precession will last forever. Moreover, when $\rho_{cck(1/2)(-1/2)}$ decays to zero, there is no electron spin precession. Therefore, we refer it as spin coherence in the following. $P_{k(-1/2)(3/2)}$ and $P_{k(1/2)(-3/2)}$, which describe the coherence between the states with the optical transition between them being forbidden by the selection rule, may play certain role in the optical dephasing and we will refer them hereafter as forbidden optical coherences. Finally, there is also a coherence between two VB's with opposite spin directions: $\rho_{vvk(3/2)(-3/2)} \equiv \langle c^\dagger_{vk(-3/2)} c_{vk(3/2)} \rangle$. In the absence of spin flip of the hh, this coherence is much weaker than the other coherences as it then can only be excited by the laser pulse through the coupling to the forbidden coherence. Therefore, in the present discussion of the undoped material, we do not include it in our model.

B. Kinetic equations

We build the semiconductor Bloch equations for the quantum well by nonequilibrium Green-function method[14] as follows:

$$\dot{\rho}_{\mu\nu,k,\sigma\sigma'} = \dot{\rho}_{\mu\nu,k,\sigma\sigma'}|_{\rm coh} + \dot{\rho}_{\mu\nu,k,\sigma\sigma'}|_{\rm scatt}. \tag{4}$$

Here $\rho_{\mu\nu,k,\sigma\sigma'}$ represents a single-particle density matrix with μ and $\nu = c$ or v. The diagonal elements describe the carrier distribution functions $\rho_{\mu\mu,k,\sigma\sigma} = f_{\mu k\sigma}$ of the band μ, the wave vector k and the spin σ. It is further noted that $f_{ck\sigma} \equiv f_{ek\sigma}$ represents the electron distribution function with $\sigma = \pm 1/2$ and $f_{vk\sigma} = 1 - f_{hk\sigma}$ with $f_{hk\sigma}$ denoting the hh distribution function and $\sigma = \pm 3/2$. The off-diagonal elements describe the interspin-band polarization components (coherences) we defined at the end of the previous subsection with $\rho_{cv,k,\sigma\sigma'} = p_{k\sigma\sigma'} = P_{k\sigma\sigma'} e^{-i\omega t}$ for the inter-CB-VB polarization and $\rho_{cc,k,(1/2)-1/2}$ for the spin coherence. It is noticed here that for $P_{k\sigma\sigma'}$, the first spin index σ always corresponds to the spin index of the electron in the CB ($\pm 1/2$) and the second spin index σ' always corresponds to that of the hh VB ($\pm 3/2$).

The coherent part of the equation of motion for the electron distribution function in the rotating wave approximation is given by

$$\begin{aligned}\left.\frac{\partial f_{ek\sigma}}{\partial t}\right|_{\rm coh} &= d\,\delta_{\sigma(1/2)} {\rm Im}[E_-^{0*}(t) P_{k\sigma(3/2)}] \\ &+ d\,\delta_{\sigma(-1/2)} {\rm Im}[E_+^{0*}(t) P_{k\sigma(-3/2)}] \\ &+ 2\sum_q V_q\, {\rm Im}\Bigg(\sum_{\sigma'} P^*_{k+q\sigma\sigma'} P_{k\sigma\sigma'} \\ &+ \rho_{cc,k+q,-\sigma\sigma} \rho_{cc,k,\sigma-\sigma} \Bigg) - g\mu_B B\, {\rm Im}\,\rho_{cc,k,\sigma-\sigma}.\end{aligned} \tag{5}$$

The first two terms describe the generation rates by the polarized laser pulses. As mentioned before, the selection rule requires that the optical transition can only happen between the conduction and the valence bands with the same spin direction. This selection rule is enforced by the Kronecker δ-function $\delta_{\sigma(\pm 1/2)}$. The third term describes the exchange interaction correction of the exciting laser by the electron-hole attraction, thus it can be seen as a local field correction of the time dependent bare Rabi frequency $dE^0_\pm(t)$. The last term describes the spin flip and flop of electrons. It is noticed that if ${\rm Im}\,\rho_{cc,k,\sigma-\sigma} = 0$, there is *no* spin flip and flop. Therefore, we call $\rho_{cc,k,\sigma-\sigma}$ spin coherence. It is further noticed that $\rho_{cc,k,(-1/2)(1/2)} = \rho^*_{cc,k,(1/2)(-1/2)}$. Similarly the coherent part of the equation of motion for the hole distribution function is written as

$$\begin{aligned}\left.\frac{\partial f_{hk\sigma}}{\partial t}\right|_{\rm coh} &= -2\sum_{q\sigma'} V_q\, {\rm Im}(P_{k+q\sigma'\sigma} P^*_{k\sigma'\sigma}) \\ &+ d\,\delta_{\sigma(3/2)} {\rm Im}[E_-(t)^* P_{k(1/2)\sigma}] \\ &+ d\,\delta_{\sigma(-3/2)} {\rm Im}[E_+(t)^* P_{k(-1/2)\sigma}].\end{aligned} \tag{6}$$

One notices here that differing from the electron distribution function, there are *no* terms like $g\mu_B B\,{\rm Im}\,\rho_{vv,k,\sigma-\sigma}$ in the coherent part of equation of motion for the hole distribution even if we do not neglect the contribution from $\rho_{vv,k,\sigma-\sigma}$. Again this is due to the fact that $(S_v^x)_{\pm 3/2,\pm 3/2} = 0$ and therefore the spin of the hole cannot be flipped. The scattering rates of $f_{ek\sigma}$ and $f_{hk\sigma}$ for the Coulomb scattering in the Markovian limit are given by

$$\left.\frac{\partial f_{ek\sigma}}{\partial t}\right|_{\text{scat}} = -2\sum_{j=e,h,k'q\sigma'} V_q^2 2\pi\delta(\varepsilon_{ek-q}-\varepsilon_{ek}+\varepsilon_{jk'}-\varepsilon_{jk'-q})\Big\{(1-f_{ek-q\sigma})f_{ek\sigma}(1-f_{jk'\sigma'})f_{jk'-q\sigma'}-f_{ek-q\sigma}$$
$$\times(1-f_{ek\sigma})f_{jk'\sigma'}(1-f_{jk'-q\sigma'})$$
$$+\Big[\sum_{\sigma''}\text{Re}(P_{k-q\sigma\sigma''}P^*_{k\sigma\sigma''})+\text{Re}(\rho_{cc,k-q,\sigma-\sigma}\rho_{cc,k,-\sigma\sigma})\Big](f_{jk'\sigma'}-f_{jk'-q\sigma'})$$
$$+\sum_{\sigma''}\text{Re}(P_{k'\sigma'\sigma''}P^*_{k'-q\sigma'\sigma''})(f_{ek-q\sigma}-f_{ek\sigma})\Big\}$$
$$-2\sum_{k'q\sigma'} V_q^2 2\pi\delta(\varepsilon_{ek-q}-\varepsilon_{ek}+\varepsilon_{ek'}-\varepsilon_{ek'-q})\rho_{cc,k',\sigma'-\sigma'}\rho_{cc,k'-q,-\sigma'\sigma'}(f_{ek-q\sigma}-f_{ek\sigma}), \tag{7}$$

and

$$\left.\frac{\partial f_{hk\sigma}}{\partial t}\right|_{\text{scat}} = 2\sum_{j=e,h,k'q\sigma'} V_q^2 2\pi\delta(\varepsilon_{hk}-\varepsilon_{hk-q}+\varepsilon_{jk'-q}-\varepsilon_{jk'})\Big\{f_{hk-q\sigma}(1-f_{hk\sigma})(1-f_{jk'-q\sigma'})f_{jk'\sigma'}$$
$$-f_{hk\sigma}(1-f_{hk-q\sigma})f_{jk'-q\sigma'}(1-f_{jk'\sigma'})$$
$$-\sum_{\sigma''}[\text{Re}(P^*_{k-q\sigma''\sigma}P_{k\sigma''\sigma})(f_{jk'\sigma'}-f_{jk'-q\sigma'})+\text{Re}(P^*_{k'-q\sigma'\sigma''}P_{k'\sigma'\sigma''})(f_{hk-q\sigma}-f_{hk\sigma})]\Big\}$$
$$+2\sum_{k'q\sigma'} V_q^2 2\pi\delta(\varepsilon_{hk}-\varepsilon_{hk-q}+\varepsilon_{ek'-q}-\varepsilon_{ek'})\rho_{cc,k'-q,\sigma'-\sigma'}\rho_{cc,k',-\sigma'\sigma'}(f_{hk\sigma}-f_{hk-q\sigma}). \tag{8}$$

One can easily prove from Eqs. (7) and (8) that $\Sigma_k \partial f_{ek\sigma}/\partial t|_{\text{scat}} = \Sigma_k \partial f_{hk\sigma}/\partial t|_{\text{scat}} = 0$. This is because the Coulomb scattering does not change the total population of each band.

The coherent time evolution of the interband polarization component is given by

$$\left.\frac{\partial}{\partial t}P_{k\sigma\sigma'}\right|_{\text{coh}} = -i\delta_{\sigma\sigma'}(k)P_{k\sigma\sigma'}-\frac{i}{2}g\mu_B B P_{k-\sigma\sigma'}+\frac{i}{2}dE_-(t)[\delta_{\sigma(1/2)}(1-f_{hk(3/2)})-\rho_{cc,k,\sigma(1/2)}]\delta_{\sigma'(3/2)}+\frac{i}{2}dE_+(t)[\delta_{\sigma(-1/2)}$$
$$\times(1-f_{hk(-3/2)})-\rho_{cc,k,\sigma(-1/2)}]\delta_{\sigma'(-3/2)}$$
$$-i\sum_q V_q[P_{k+q,\sigma\sigma'}(1-f_{hk\sigma'}-f_{ek\sigma})$$
$$-P_{k+q,-\sigma\sigma'}\rho_{cc,k,\sigma-\sigma}+\rho_{cc,k+q,\sigma-\sigma}P_{k,-\sigma\sigma'}]. \tag{9}$$

The first term gives the free evolution of the polarization components with the detuning

$$\delta_{\sigma\sigma'}(k) = \varepsilon_{ek}+\varepsilon_{hk}-\Delta_0-\sum_q V_q(f_{ek+q\sigma}+f_{hk+q\sigma'}) \tag{10}$$

and $\Delta_0 = \omega - E_g$. Δ_0 is the detuning of the center frequency of the light pulses with respect to the unrenormalized band gap. The second term in Eq. (9) describes the coupling of the optical coherence $P_{k\sigma\sigma}$ with the forbidden optical coherences $P_{k\sigma-\sigma}$ and $P_{k-\sigma\sigma}$ due to the presence of the magnetic field B. This coupling makes $P_{k\sigma-\sigma}$ and $P_{k-\sigma\sigma}$ not small enough to be neglected in our calculation. The last term in Eq. (9) describes again the excitonic correlations. The coherent time evolution of the spin coherence is given by

$$\left.\frac{\partial}{\partial t}\rho_{cc,k,\sigma-\sigma}\right|_{\text{coh}} = \frac{i}{2}d(\delta_{\sigma(1/2)}E_-(t)P^*_{k-\sigma(3/2)}-\delta_{-\sigma(1/2)}E_-(t)^*P_{k\sigma(3/2)})+\frac{i}{2}d(\delta_{\sigma(-1/2)}E_+(t)P^*_{k-\sigma(-3/2)}$$
$$-\delta_{-\sigma(-1/2)}E_+(t)^*P_{k\sigma(-3/2)})+i\sum_q V_q[(f_{ek+q\sigma}-f_{ek+q-\sigma})\rho_{cc,k,\sigma-\sigma}-\rho_{cc,k+q,\sigma-\sigma}(f_{ek\sigma}-f_{ek-\sigma})$$
$$+P_{k+q\sigma\sigma_1}P^*_{k-\sigma\sigma_1}-P^*_{k+q-\sigma\sigma_1}P_{k\sigma\sigma_1}]+\frac{i}{2}g\mu_B B(f_{ek\sigma}-f_{ek-\sigma}). \tag{11}$$

One notices from both the last terms of Eqs. (5) and (11) that the spin coherence causes the electrons oscillating between the spin-up and spin-down bands and in the mean time the unbalance between these two bands feeds back to the spin coherence. It is further noted from the first two terms of Eq. (11) that pump pulse also generates the spin coherence. However, as this process is through the coupling to the forbidden transitions, its contribution is negligible compared to the effect due to magnetic field [last term of Eq. (11)] as will be shown in the later sections.

The dephasing of the interband polarization components is determined by the following scattering:

$$\left.\frac{\partial P_{k\sigma\sigma_0}}{\partial t}\right|_{\text{scat}} = \Bigg\{ -\sum_{\substack{j=e,h\\ k'q\sigma'}} V_q^2 2\pi\delta(\varepsilon_{ek-q}+\varepsilon_{hk}+\varepsilon_{jk'}-\varepsilon_{jk'-q}-\Delta_0)\Bigg\{(P_{k,\sigma\sigma_0}-P_{k-q,\sigma\sigma_0})\Bigg[(1-f_{jk'\sigma'})f_{jk'-q\sigma'}$$
$$-\sum_{\sigma''} P_{k',\sigma'\sigma''}P^*_{k'-q,\sigma'\sigma''}\Bigg]+(\rho_{cc,k-q,\sigma-\sigma}P_{k,-\sigma\sigma_0}+f_{ek-q\sigma}P_{k\sigma\sigma_0}-f_{hk\sigma_0}P_{k-q\sigma\sigma_0})(f_{jk'\sigma'}-f_{jk'-q\sigma'})\Bigg\}$$
$$+\sum_{k'q\sigma'} V_q^2 2\pi\delta(\varepsilon_{ek-q}+\varepsilon_{hk}+\varepsilon_{ek'}-\varepsilon_{ek'-q}-\Delta_0)(P_{k\sigma\sigma_0}-P_{k-q\sigma\sigma_0})\rho_{cc,k',\sigma'-\sigma'}\rho_{cc,k'-q,-\sigma'\sigma'}\Bigg\}$$
$$-\{k\leftrightarrow k-q,k'\leftrightarrow k'-q\}-\frac{P_{k\sigma\sigma_0}}{T_2}. \tag{12}$$

Here, T_2 is introduced phenomenologically to describe additional slower scattering process such as carrier-phonon scattering. $\{k\leftrightarrow k-q,k'\leftrightarrow k'-q\}$ in Eq. (12) stands for the same terms as in the previous $\{\ \}$ but with the interchanges $k\leftrightarrow k-q$ and $k'\leftrightarrow k'-q$. We point out here that all the scattering terms in Eqs. (7), (8), and (12) are the contributions from the Coulomb scattering. We did not include the EHSE scatterings as they are much weaker in comparison with the Coulomb scatterings.

The Coulomb scattering contribution to the scattering term of the spin coherence is

$$\left.\frac{\partial \rho_{cc,k\sigma-\sigma}}{\partial t}\right|^{\text{Coul}}_{\text{scat}} = \Bigg(-\sum_{\substack{j=e,h\\ qk'\sigma'}} V_q^2 2\pi\delta(\varepsilon_{ek-q}-\varepsilon_{ek}+\varepsilon_{jk'}-\varepsilon_{jk'-q})\Bigg\{\Bigg(f_{ek-q\sigma}\rho_{cc,k,\sigma-\sigma}+\rho_{cc,k-q,\sigma-\sigma}f_{ek-\sigma}$$
$$+\sum_{\sigma''} P_{k-q\sigma\sigma''}P^*_{k-\sigma-\sigma''}\Bigg)(f_{jk'\sigma'}-f_{jk'-q\sigma'})+\rho_{cc,k,\sigma-\sigma}\Bigg[(1-f_{jk'\sigma'})f_{jk'-q\sigma'}-\sum_{\sigma''} P_{k'\sigma'\sigma''}P^*_{k'-q\sigma'\sigma''}$$
$$-\delta_{j=e}\rho_{cc,k',\sigma'-\sigma'}\rho_{cc,k'-q,-\sigma'\sigma'}\Bigg]-\rho_{cc,k-q,\sigma-\sigma}\Bigg[f_{jk'\sigma'}(1-f_{jk'-q\sigma'})-\sum_{\sigma''} P_{k'\sigma'\sigma''}P^*_{k'-q\sigma'\sigma''}$$
$$-\delta_{j=e}\rho_{cc,k',\sigma'-\sigma'}\rho_{cc,k'-q,-\sigma'\sigma'}\Bigg]\Bigg\}\Bigg)-\{k\leftrightarrow k-q,k'\leftrightarrow k'-q\}. \tag{13}$$

One can prove from Eq. (13) analytically that

$$\sum_k \left.\frac{\partial \rho_{cc,k\sigma-\sigma}}{\partial t}\right|^{\text{Coul}}_{\text{scat}} = 0. \tag{14}$$

This can be easily seen as the second half of Eq. (13) comes from the first half by interchanging $k\leftrightarrow k-q$ and $k'\leftrightarrow k'-q$. In the sum over k of Eq. (14), one may perform the following variable transformations: $k\rightarrow -k+q$ and $k'\rightarrow -k'+q$ to the second half of Eq. (13), which make the second half just the same as the first one but with opposite sign. Equation (14) indicates that the Coulomb scattering does not contribute to the spin dephasing.

In order to study the dephasing of the spin coherence, we pick up the contributions from EHSE scattering. The ''direct'' EHSE contribution is given by

$$\left.\frac{\partial \rho_{cc,k\sigma-\sigma}}{\partial t}\right|^{\text{dEHSE}}_{\text{scat}} = \Bigg\{ -\frac{9}{16}\sum_{k'q\sigma'} U_q^2 2\pi\delta(\varepsilon_{ek-q}-\varepsilon_{ek}-\varepsilon_{hk'}+\varepsilon_{hk'-q})[(2-f_{ek\sigma}-f_{ek-\sigma})\rho_{cc,k-q,\sigma-\sigma}f_{hk'-q\sigma'}(1-f_{hk'\sigma'})$$
$$+\rho_{cc,k,\sigma-\sigma}(f_{ek-q\sigma}+f_{ek-q-\sigma})f_{hk'-q\sigma'}(1-f_{hk'\sigma'})]\Bigg\}+\{k\leftrightarrow k-q,k'\leftrightarrow k'-q\}. \tag{15}$$

The ''exchange'' EHSE contribution can be written as

$$\left.\frac{\partial \rho_{cc,k\sigma-\sigma}}{\partial t}\right|_{\text{scat}}^{\text{eEHSE}} = \Bigg\{ -\frac{9}{16}\sum_{k'q\sigma'} U'^{2}_{q} 2\pi\delta(\varepsilon_{ek'}+\varepsilon_{hk'-q}-\varepsilon_{ek}-\varepsilon_{hk-q})[(2-f_{ek'\sigma}-f_{ek'-\sigma})\rho_{cc,k,\sigma-\sigma}f_{hk-q\sigma'}(1-f_{hk'-q\sigma'}) + \rho_{cc,k',\sigma-\sigma}(f_{ek\sigma}+f_{ek-\sigma})f_{hk-q\sigma'}(1-f_{hk'-q\sigma'})] \Bigg\} + \{k\leftrightarrow k'\}. \tag{16}$$

It is noted that in Eqs. (15) and (16), the second half of each equation shares the same sign as the first half. Therefore, $\Sigma_k \partial\rho_{cc,k\sigma-\sigma}/\partial t|_{\text{scat}}^{\text{dEHSE}} \neq 0$ and $\Sigma_k \partial\rho_{cc,k\sigma-\sigma}/\partial t|_{\text{scat}}^{\text{eEHSE}} \neq 0$. This tells us that EHSE contributes to the spin dephasing. One further finds by comparing Eqs. (15) and (16) that besides the above mentioned $U'_q \ll U_q$, the energy phase space of the ''exchange'' EHSE, which is imposed by the energy conservation, is quite limited compared to that of ''direct'' EHSE. All these indicate that the contribution of the ''exchange'' EHSE is negligible in comparison with that of the ''direct'' EHSE. We have further proved that there is *no* contribution to the scattering term from the combination of Coulomb scattering and EHSE as U_qV_q or U'_qV_q. Therefore,

$$\left.\frac{\partial \rho_{cc,k\sigma-\sigma}}{\partial t}\right|_{\text{scat}} = \left.\frac{\partial \rho_{cc,k\sigma-\sigma}}{\partial t}\right|_{\text{scat}}^{\text{Cou}} + \left.\frac{\partial \rho_{cc,k\sigma-\sigma}}{\partial t}\right|_{\text{scat}}^{\text{dEHSE}} + \left.\frac{\partial \rho_{cc,k\sigma-\sigma}}{\partial t}\right|_{\text{scat}}^{\text{eEHSE}}. \tag{17}$$

Equations (4)–(17) comprise the complete set of kinetic equations. It is noted that we only include EHSE in the scattering term of the spin coherence. Its contribution to the optical coherences and electron (hole) distributions are neglected as it is much smaller than the contribution from the Coulomb scattering.[23] Moreover, the electron-hole recombination is not included in our model as the time scale for such an effect is at least one order of magnitude longer than the time scale of dephasing.

C. Faraday rotation angle

The FR angle can be calculated for two degenerate Gaussian pulses with variable delay time τ. The first pulse (pump) is circular polarized, e.g., $E^0_{\text{pump}} = E^0_-(t)$, and travels in the direction $\mathbf{k}_1$. The second pulse (probe) is linear polarized and is much weaker than the first one, e.g., $E^0_{\text{prob}}(t) = E^0_{\text{prob},-}(t-\tau) + E^0_{\text{prob},+}(t-\tau) \equiv \chi[E^0_-(t-\tau) + E^0_+(t-\tau)]$ with $\chi \ll 1$. The probe pulse travels in the $\mathbf{k}_2$ direction.

The FR angle is defined as[19,24]

$$\Theta_F(\tau) = C\sum_k \int \text{Re}[\overline{P}_{k(1/2)(3/2)}(t)E^{0*}_{\text{prob},-}(t-\tau) - \overline{P}_{k(-1/2)(-3/2)}(t)E^{0*}_{\text{prob},+}(t-\tau)]dt, \tag{18}$$

with $\overline{P}_{k\sigma\sigma}$ standing for the optical transition in the prob direction, i.e., $\mathbf{k}_2$ direction. C is a constant.

For the delay time τ is shorter than the optical dephasing time, one has to project the optical transition $P_{k\sigma\sigma}$ to $\mathbf{k}_2$ direction. One may use an adiabatic projection technique described in detail in Ref. 25. This technique is suitable for optically thin crystals, where the spatial dependence can be treated adiabatically.[26] To do so, one replaces the single-pulse envelope function in Eqs. (5) and (6) by two delayed pulses $E^0_-(t) = E^0_-(t)e^{i\varphi} + E^0_{\text{prob},-}(t-\tau)$ and $E^0_+(t) = E^0_{\text{prob},+}(t-\tau)$ with the relative phase $\varphi = (\mathbf{k}_1 - \mathbf{k}_2)\cdot\mathbf{x}$ resulting from the different propagation directions. The projection technique is used with respect to this phase. However, when delay time τ is much longer than the optical dephasing, the optical transition $P_{k\sigma\sigma}$ induced by the pump pulse has already decayed to zero and therefore one may perform the calculation with $\varphi \equiv 0$.

It is interesting to see from Eq. (18) that although the spin coherence is determined by $\rho_{cc,k,(1/2)(-1/2)}$, it does not appear directly in the final equation of the FR angle. Instead, it affects the FR angle through the optical transitions $P_{k\sigma\sigma}$. For delay time τ much longer than the optical dephasing time, the optical coherences $P_{k\sigma\sigma}$ induced directly by the pump pulse together with the forbidden optical coherences $P_{k\sigma-\sigma}$ have already been destroyed to zero. However, the spin coherence induced by the same pump pulse remains and makes the electrons oscillate between the spin-up and -down bands. This unbalance of population strongly affects the optical transitions induced later by the probe pulse around τ and gives rise to the time evolution of Faraday rotation angle.

III. NUMERICAL RESULTS

We perform a numerical study of the Bloch equations to study the spin coherence of optically excited electrons in an undoped insulating $ZnSe/Zn_{1-x}Cd_xSe$ quantum well. As the main interest of the present paper is focused on the mechanism of the spin dephasing, we will not perform a pump-probe computation to calculate the FR angle Eq. (18) as it requires extensive CPU time and also as it has been calculated by Linder and Sham[19] for the same set of Bloch equations but with relaxation time approximation for all the dephasing. Instead, we will only apply a single pump pulse and calculate the time evolutions of both the optical and spin coherences together with the electron and hh distributions after that pulse under the carrier-carrier scattering. The dephasing of the spin coherence is well defined by the incoherently-summed spin coherence, $\rho(t) = \Sigma_k|\rho_{cc,k,(1/2)(-1/2)}(t)|$, as well as the optical dephasing is described by the incoherently summed polarization, $P_{\sigma\sigma}(t) = \Sigma_k|P_{k,\sigma\sigma}(t)|$. The latter was first introduced by Kuhn and Rossi.[30] It is understood that both true dissipation and the interference of many k states may contribute to the decay. The incoherent summation is therefore used to isolate the irreversible decay from the decay caused by interference. From $\rho(t)$ and $P_{\sigma\sigma}(t)$ one gets the true irreversible dephas-

ing of spin and optical coherences, respectively.

The material parameters in our calculation are taken from the experimental data with effective mass $m_e=0.152m_0$ for electron[27] and $m_h=6m_e$ for hh.[28] Exciton Rydberg $E_R=19$ meV and the g factor is taken as 1.3. This g factor is larger than that reported in the experiment[11] (1.1) by measuring the beat frequency of the FR angle. The reason will be shown clearly in later subsections. T_2 is taken as 10 ps for all the calculations. We choose a left circular polarized Gaussian pulse $E_-^0(t)$ with the width $\delta t=100$ fs and detuning $\Delta_0=4.275$ meV. The total density excited by this pulse is 3×10^{11} cm^{-2}, which is the same as that reported in the experiment.[11] $E_+^0(t)\equiv0$. Under such a pulse, one can see immediately from the kinetic equations that only hh with spin $3/2$ can be excited and $f_{hk(-3/2)}\equiv0$. Moreover, $P_{k(-1/2)(-3/2)}=P_{k(1/2)(-3/2)}\equiv0$. Therefore, we only need to determine the electron distribution functions $f_{ek\sigma}$ $(\sigma=\pm1/2)$, the hh distribution functions $f_{hk(3/2)}$, interband polarizations (optical coherences) $P_{k(1/2)(3/2)}$ and $P_{k(-1/2)(3/2)}$, and spin coherences $\rho_{cc(1/2)(-1/2)}$. We will solve the Bloch equations with only Coulomb scattering and with both Coulomb scattering and EHSE scatterings, respectively.

A. Coulomb scattering

We first discuss the Boltzmann kinetics under the Coulomb scattering with the statically screened instantaneous potential approximation

$$V_q=\frac{2\pi e^2}{\epsilon_0(q+\kappa)}. \tag{19}$$

The inverse screening length κ is expressed as[29,14]

$$\kappa(t)=\frac{m_e e^2}{\epsilon_0}\sum_\sigma\left[f_{ek=0\sigma}(t)+\frac{m_h}{m_e}f_{hk=0\sigma}(t)\right]. \tag{20}$$

It is noted that this static screening model, although simplifying numerical calculation significantly, overlooks the plasmon-mode contributions and overestimates the electron screening.

We first show in Fig. 1 the electron and hole distribution functions $f_{ek\sigma}(t)(\sigma=\pm1/2)$ and $f_{hk(3/2)}(t)$ versus t and electron energy ε_{ek} (for electron distributions) or hh energy ε_{hk} (for hole distribution) for $B=4$ T. In the initial time one observes a small peak around 10 meV for $f_{ek(1/2)}$ in Fig. 1(a). This peak is the effect of the pump pulse and strong Hartree correction Eq. (10). The similar peak can also be observed for the hh distribution function in Fig. 1(c). At later times the carriers relax to the low-energy states and $f_{ek(1/2)}$ reaches its first highest peak at 1.4 ps. Around 7 ps, the distribution function of spin-up band reaches the valley of zero values and the spin-down band, in the mean time, arrives at its peak. This indicates that electrons in the spin-up band evolve into the spin-down band. After that electrons start to move back to the spin-up band and at about 14 ps $f_{ek(1/2)}$ reaches its second highest peak and $f_{ek(-1/2)}$ reaches its valley. The reason that the second highest peak is a little higher than the first one is because there are more electrons at higher energy states at initial times due to the position of the pump pulse. This oscillation keeps going without any decay. The distribution for hh relaxes into the Fermi-like distribution after a few picoseconds and remains unchanged. In Fig. 2, the absolute value of the optical coherence, $|P_{k,(1/2)(3/2)}(t)|$, and the absolute value of the spin coherence, $|\rho_{cc,k,(1/2)(-1/2)}(t)|$, are plotted as functions of t and electron energy. It is seen from Fig. 2(a) that the optical coherence decays very quickly and within the first few picoseconds it has already totally disappeared. Nevertheless, the

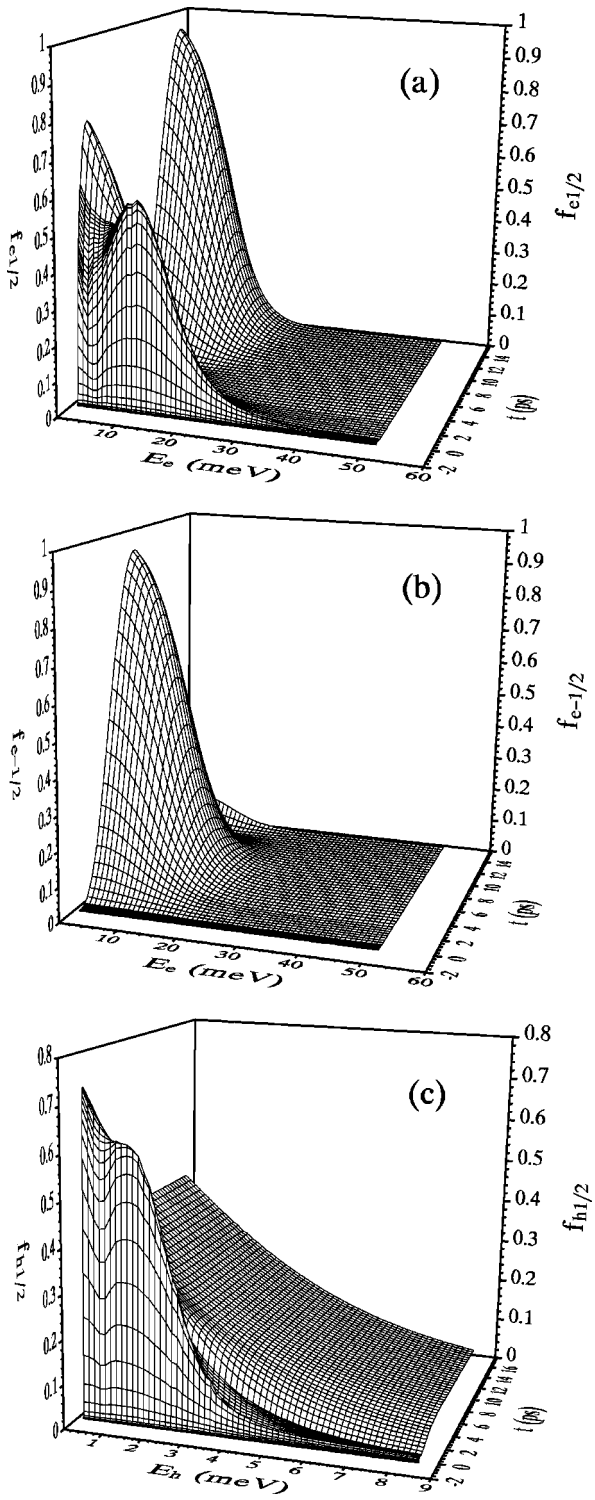

FIG. 1. Electron distributions vs time t and electron energy E_e for the spin 1/2 [Fig. 1(a)] and $-1/2$ [Fig. 1(b)] and hh distribution vs t and hh energy E_h [Fig. 1(c)].

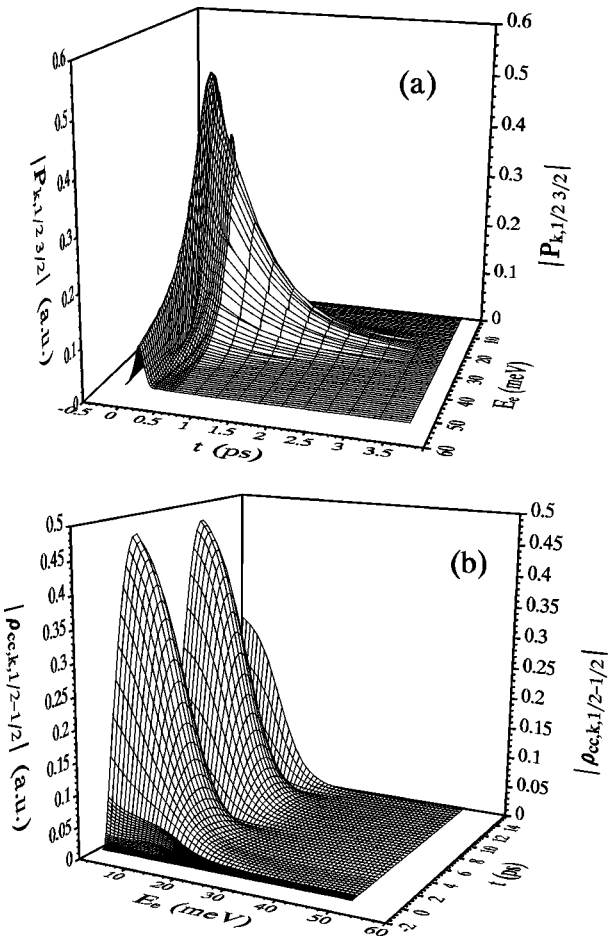

FIG. 2. Absolute amounts of optical coherence $|P_{k(1/2)(3/2)}(t)|$ [Fig. 2(a)] and spin coherence $|\rho_{cc,k,(1/2)(-1/2)}(t)|$ [Fig. 2(b)] as functions of t and electron energy E_e. Note the time scale of optical coherence is much shorter than the spin coherence.

spin coherence does not decay at all. The second peak is of the same height as the first one.

The incoherently summed polarization, $P_{(1/2)(3/2)}(t)$, and the incoherently summed spin coherence, $\rho(t)$, are plotted as dashed curves in Fig. 3. The total densities of each spin band $N_{e\sigma}(t)=\Sigma_k f_{ek\sigma}(t)$ for electron and $N_{h(3/2)}(t)=\Sigma_k f_{hk(3/2)}(t)$ for hh are also plotted as solid curves in the same figure. It is seen from the figure that the optical coherence injected by the pump pulse is about 3 times larger than the spin coherence. However, this coherence is strongly dephased by the Coulomb scattering and is totally gone within the first few picoseconds. It is further shown from the figure that the spin coherence exhibits beating that does not decay at all. The electron densities of spin-up and down bands oscillate between zero and the total excitation. These results confirm that pure Coulomb scattering does not contribute to the spin dephasing. We further find that the frequency of the oscillation is mainly determined by the Zeeman split $g\mu_B B$, but redshifted by the Hartree-Fock terms in Eq. (11). The reduced g factor resulting from the oscillation frequency is 1.25. It is interesting to see from the figure that the maximum value of $|N_{e(1/2)}-N_{e(-1/2)}|$ occurs when the (incoherently summed) spin coherence is zero. The forbidden optical coherence is about 30 times smaller than the

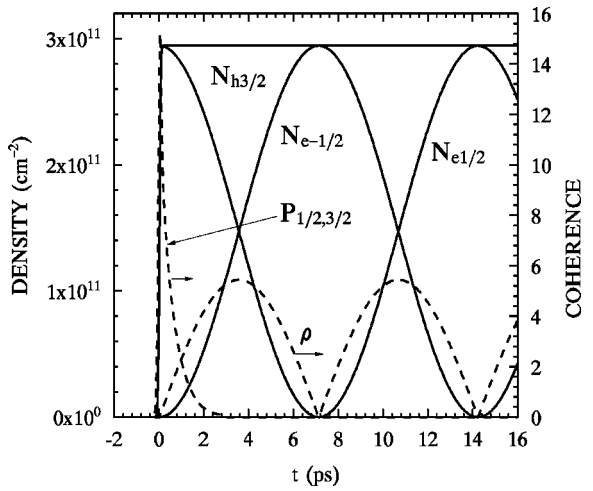

FIG. 3. Total densities of each spin band $N_{ek\sigma}(t)$ for electron and $N_{hk(3/2)}(t)$ for hh (solid curves) together with the incoherently summed polarization $P_{(1/2)(3/2)}$ and spin coherence $\rho(t)$ (dashed curves) are plotted against time t for $B=4$ T. Note the scale of the coherences is on the right side of the figure.

optical coherence and decays similarly as the optical coherence. It plays an insignificant role in this problem.

B. EHSE

Now we include the contribution of EHSE [Eqs. (15) and (16)]. As said before that the contribution from ''exchange'' EHSE is negligible, we therefore only include the ''direct'' one [Eq. (15)] here. We are lacking information of the matrix elements U_q, which requires a detailed band-structure calculation. For the sake of simplicity and also for comparison with the effect of Coulomb scattering, in this study we assume it is the same as V_q but with a phenomenological prefactor $4\sqrt{\mathcal{F}}/3$. We take $\mathcal{F}=0.015$ so that in the scattering term, Eq. (15), the matrix element of EHSE is two orders of magnitude smaller than that of the Coulomb scattering. This number is taken so that the spin dephasing time is in agreement with the experiment.[11] We have also performed numerical calculation by taking only the ''exchange'' EHSE and found in order to get the same spin dephasing, the prefactor has to be 0.1, which is one order of magnitude larger than the present case. This big prefactor is understood due to the effect of the limitation of the energy phase space discussed before.

The electron distribution functions $f_{ek\sigma}(t)(\sigma=\pm 1/2)$ versus t and electron energy ε_{ek} are plotted in Fig. 4 for $B=4$ T. The hh distribution function $f_{hk(3/2)}(t)$ versus t and hh energy ε_{hk} remains unchanged from Fig. 1(c) after the inclusion of EHSE. In the initial time one observes again a small peak around 10 meV for $f_{ek(1/2)}$ in Fig. 4(a) due to the effect of pump detuning. A similar peak can also be observed for the hh distribution function as in Fig. 1(c). Again one observes that the carriers relax at later times to the low-energy states and all the distributions show the Fermi-like distributions. Differing from the case with only Coulomb scattering, there are only small oscillations of electrons between spin 1/2 and $-1/2$ bands in the later time. The hh distribution remains unchanged after the first few picoseconds as before. The absolute value of optical coherence,

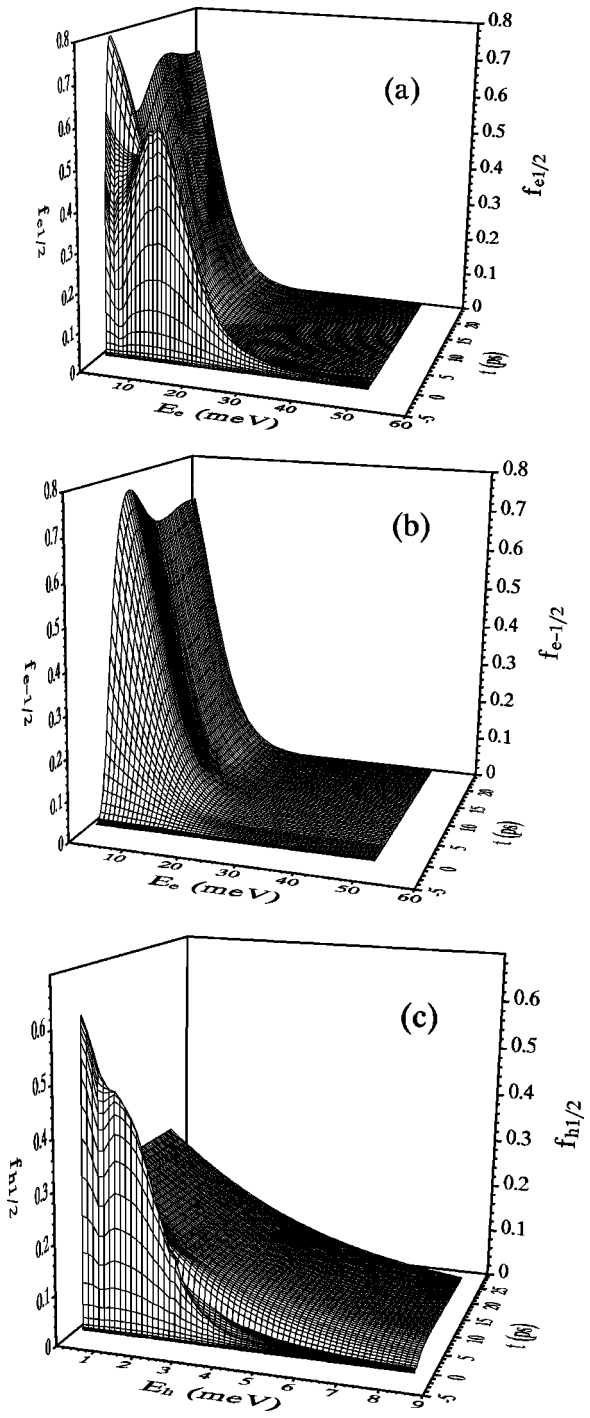

FIG. 4. Electron distributions vs time t and electron energy E_e for the spin 1/2 [Fig. 4(a)] and $-1/2$ [Fig. 4(b)] and hh distribution vs t and hh energy E_h [Fig. 4(c)] for $B=4$ T. Effects of EHSE are included.

$|P_{k(1/2)(3/2)}(t)|$ [Fig. 5(a)], versus t and electron energy is also unchanged from Fig. 2(a) after inclusion of EHSE. Therefore, as before, the optical coherence decays very quickly and within a few picoseconds it has totally disappeared. However, EHSE makes a big change to the absolute value of the spin coherence as can be seen in Fig. 5(b) where $|\rho_{cc,k,(1/2)-1/2}(t)|$ is plotted as a function of t and electron energy. It is seen that the spin coherence lasts much longer and one can see a smaller second peak around 10.5 ps and a

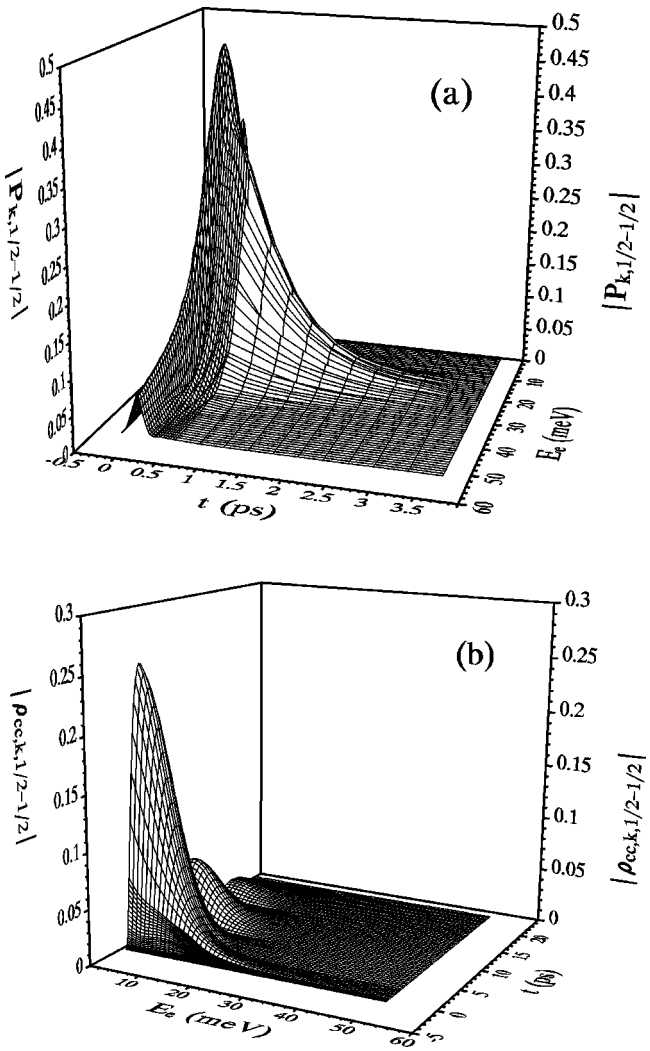

FIG. 5. Absolute amounts of optical coherence $|P_{k(1/2)(3/2)}(t)|$ [Fig. 5(a)] and spin coherence $|\rho_{cc,k,(1/2)-1/2}(t)|$ [Fig. 5(b)] as functions of t and electron energy E_e. Effects of EHSE are included. $B=4$ T.

much smaller third peak around 18.4 ps. Comparing with Fig. 2(b), one can see the effect of strong spin-dephasing by EHSE as the second peak is much lower than the first one. For $t>20$ ps, the spin coherence has almost gone. One more that point needing to be addressed here is, as one can see from Fig. 5(b), there is a very small bump around 10 meV at initial time. A similar bump can also be seen in Fig. 2(b). These bumps are the effects of the pump pulse described before after Eq. (11). One can see that they are much smaller compared to the effects caused by the magnetic field. This also justifies the assumption we made before that hh-hh spin coherence can be neglected in this investigation.

The incoherently summed polarization, $P_{(1/2)(3/2)}(t)$, and the incoherently summed spin coherence, $\rho(t)$, are plotted as dashed curves in Fig. 6. In order to have the effect of spin coherence more pronounced, we plot in the same figure also $4.5\times\rho(t)$ as dash-dotted curve. The total densities of each spin band $N_{e\sigma}(t)$ and $N_{h(3/2)}(t)$ are also plotted as solid curves in Fig. 6. It is seen from the figure that the optical coherence injected by the pump pulse is about 4.5 times larger than the spin coherence. However, this coherence is strongly destroyed by the Coulomb scattering within the first

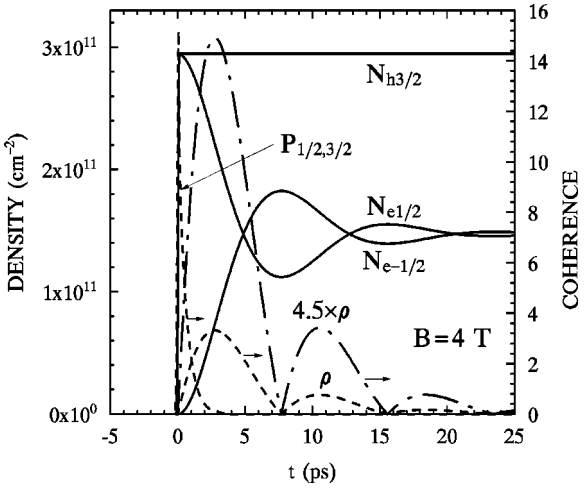

FIG. 6. Total densities of each spin band $N_{ek\sigma}(t)$ for electron and $N_{hk(3/2)}(t)$ for hh (solid curves) together with the incoherently summed polarization $P_{(1/2)(3/2)}$ and spin coherence $\rho(t)$ (dashed curves) are plotted against time t for $B=4$ T. The dash-dotted curve is $4.5\rho(t)$. Effects of EHSE are included. Note the scale of coherences is on the right side of the figure.

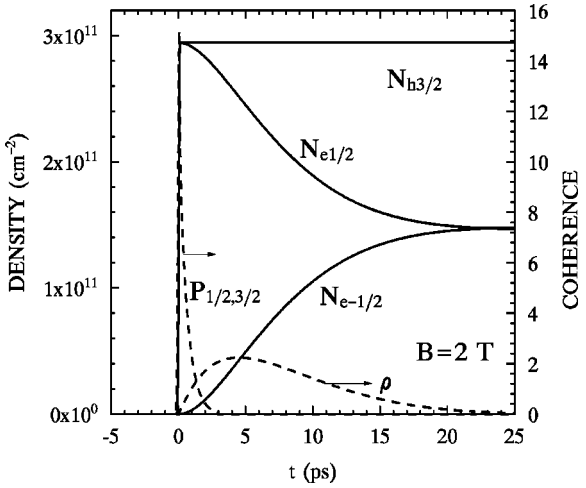

FIG. 7. Total densities of each spin band $N_{ek\sigma}(t)$ for electron and $N_{hk(3/2)}(t)$ for hh (solid curves) together with the incoherently summed polarization $P_{(1/2)(3/2)}$ and spin coherence $\rho(t)$ (dashed curves) are plotted against time t for $B=2$ T. Effects of EHSE are included. Note the scale of coherences is on the right side of the figure.

few picoseconds. This is part of the reason of the fast decay in the FR angle for the first few picoseconds in the experiment.[11] As seen in Eq. (18), the FR angle is proportional to the ''total'' optical transitions. For the first few picoseconds, the optical transitions are induced by both the pump pulse and the much weaker probe pulse, and the fast decay of the initial pump pulse-induced optical transition gives rise to the strong decay of the FR angle.

It is further shown from the figure that the electron densities of spin-up and -down bands oscillate with the amplitude of the oscillation decaying. The circularly polarized pump pulse first pumps electrons into the spin-up CB from the spin-up hh band. Therefore, electrons first occupy the spin-up CB band and leave behind hhs in the spin-up VB. Therefore, $N_{e(1/2)}$ and $N_{h(3/2)}$ fast rise to 3×10^{11} cm^{-2} within the time scale of the pump pulse. Then due to the magnetic field, electrons in the spin-up band start to go to the spin-down band. This makes $N_{e(1/2)}$ decrease and $N_{e-1/2}$ rise. In the mean time, the unbalance in populations also serves as pump field to the spin coherence. After t is around 5 ps, the electron population in the spin-down band surpasses that in the spin-up band. Without dephasing, this oscillation may keep going on as shown in the previous section. However, the spin dephasing makes these two populations finally merge. From the figure, one can see that for $t>20$ ps, the difference is already negligible compared to the oscillations before and ρ also decays to zero. This oscillation is also shown in the experiment through the FR angle as beatings for the same magnetic field.[11] All these results confirm what we proposed in Sec. II, that the spin dephasing is caused by EHSE and the electron spin coherence is represented by ρ. Moreover, one also finds that besides the effect of spin dephasing, EHSE also changes the oscillation frequency and hence the beating frequency of the FR angle. By comparing the period of the oscillations in Figs. 3 and 6, one finds the period increases by about 1.34 ps in the later case. This means that the EHSE further redshifts the spin splitting. Therefore, the g factor reported in the experiment[11] by measuring the frequency of the beating of the FR angle is the *effective g* factor. It is seen from the figure that the period of the oscillation is $T=15.58$ ps. As $2\pi/T=g_{\rm eff}\mu_B B$, the effective g factor $g_{\rm eff}$ is therefore 1.14, in agreement with that reported in the experiment as 1.1.[11] Again from the figure one observes that the maximum value of $|N_{e(1/2)}-N_{e(-1/2)}|$ occurs when the (incoherently summed) spin coherence is zero. Our calculation shows again that the forbidden optical coherence is insignificant in this problem.

In order to compare with $B=2$ T case, we plot in Fig. 7 the incoherently summed polarization $P_{(1/2)(3/2)}(t)$ and spin coherence $\rho(t)$ as function of time t, together with the total densities of each spin band $N_{e\sigma}(t)$ and $N_{h(3/2)}(t)$. One finds the spin coherence decays at the same rate as in the $B=4$ T case but without any beating. So do the electrons in the spin bands. This confirms the finding in the experiment that there is no beating in the Faraday rotation angle.[11]

IV. CONCLUSION AND DISCUSSION

In conclusion, we have performed theoretical studies of the kinetics of the spin coherence of optically excited electrons in an undoped insulating $ZnSe/Zn_{1-x}Cd_xSe$ quantum well under moderate magnetic fields in the Voigt configuration. Based on a two spin-band model in both the CB and the VB, we build the kinetic equations combined with intra- and interband Coulomb scattering and interband EHSE in the Boltzmann limit. We include all the coherences induced directly by the laser pulse—optical transitions—and indirectly through the effect of the magnetic field—electron-electron spin coherence and forbidden optical coherence—for the electron and hh in our model. The hh-hh spin coherence $\rho_{vv,k,(3/2)(-3/2)}$ is neglected in our present investigation because it cannot be induced by the effect of the magnetic field, but only through the pump pulse coupled to the forbidden transitions and is therefore much smaller than the other coherences. We separate the spin coherence from the well known optical coherences and study the effects of Coulomb

scattering and EHSE on all the coherences. We find that the Coulomb scattering makes strong dephasing of the optical coherence and forbidden optical coherence. However, it does not contribute to the spin dephasing at all. EHSE is the main mechanism leading to the spin decoherence. We numerically solve the kinetic equations for two different magnetic fields. We find that the beating in the Faraday rotation angle is basically determined by the electron Zeeman splitting $g\mu_B B$, however, with a redshift from the Coulomb Hartree-Fock contribution and EHSE effect. The forbidden optical coherence is found of marginal importance in this problem. The matrix element of the Coulomb scattering is taken as statically screened Coulomb potential and the matrix element of EHSE is assumed the same as the Coulomb scattering with a phenomenological prefactor. By fitting this prefactor with the dephasing time in the experiment,[11] our theory can well explain the experimental data for two different magnetic fields. A first principal investigation of the EHSE scattering matrix element is definitely important for a more thorough understanding of the spin dephasing.[21,22]

For the *n*-doped material, things are quite different from the undoped case discussed in this paper. Due to the presence of large numbers of doped electrons (about one order of magnitude larger than the optically excited carriers) in the CB, the lifetime of holes is therefore quite short and is measured smaller than 50 ps compared to the lower limit of 100 ps for the insulating sample.[11] The experiments found that the spin dephasing for the doped sample is three orders of magnitude longer than the undoped sample, but with a fast dephasing (losing about 50% coherence) within the first 50 ps. The fast dephasing in the initial times can be well understood by the EHSE discussed above, but modified with the fast decreasing of hh population. Nevertheless, the mechanism of the spin dephasing discussed above cannot be applied to the doped case after 50 ps as shown from Eq. (15) that the scattering of EHSE is proportional to the hole distribution and therefore its contribution to the spin dephasing decreases with the recombination of electron and hole. However, for the *n*-doped case, it is also possible for EHSE to contribute to the spin dephasing. As the timescale of the spin dephasing for the *n*-doped sample is much longer than the insulating sample, the coupling between the hh and the light hole cannot be neglected and the spin of hh also experiences the precession.[31] Therefore, the hh-hh spin coherence $\rho_{vv,k,(3/2)(-3/2)}$, which is insignificant for the undoped case, may play an important role in the doped sample. Its contribution to the scattering term to the electron spin coherence is in the similar form as Eq. (15) but all the hole distribution parts are replaced by terms composed of hh-hh spin coherences. In the absence of the hole distribution, it becomes the leading mechanism from the contribution of EHSE to the spin dephasing. Physically this contribution is the spin exchange between electrons and virtual holes. This mechanism, together with other spin dephasing mechanisms due to the band mixing for the *n*-doped case,[32] is still under investigation. A corresponding extension of the present theory for the *n*-doped material will be published in a separate paper.

ACKNOWLEDGMENTS

MWW would like to thank Professor L.J. Sham for bringing this topic into his attention and Professor A. Imamoglu and Dr. Yutaka Takahashi for valuable discussions. Dr. J.M. Kikkawa is acknowledged for providing information about his pertinent experimental work and critical reading of this manuscript. This research was supported in part by QUEST, the NSF Science and Technology Center for Quantized Electronic Structures, Grant No. DMR 91-20007, and by the National Science Foundation under Grant No. CHE 97-09038 and CDA96-01954, and by Silicon Graphics Inc.

*Author to whom correspondence should be addressed. Electronic address: mwu@chem.ucsb.edu

[1] *Proceedings of the Third International Workshop on Nonlinear Optics and Excitation Kinetics in Semiconductors, Bad Honnef, Germany* [Phys. Status Solidi B **173**, 11 (1992)].

[2] J. Shah, *Ultrafast Spectroscopy of Semiconductors and Semiconductor Microstructures* (Springer, Berlin, 1996).

[3] *Ultrafast Phenomena XI*, edited by T. Elsaesser *et al.* (Springer, Berlin, 1998).

[4] T. C. Dammen, L. Vina, J. E. Cunningham, J. Shah, and L. J. Sham, Phys. Rev. Lett. **67**, 3432 (1991).

[5] J. Wagner, H. Schneider, D. Richards, A. Fischer, and K. Ploog, Phys. Rev. B **47**, 4786 (1993).

[6] J. J. Baumberg, S. A. Crooker, D. D. Awschalom, N. Samarth, H. Luo, and J. K. Furdyna, Phys. Rev. Lett. **72**, 717 (1994); Phys. Rev. B **50**, 7689 (1994).

[7] A. P. Herberle, W. W. Rühle, and K. Ploog, Phys. Rev. Lett. **72**, 3887 (1994).

[8] C. Buss, R. Frey, C. Flytzanis, and J. Cibert, Solid State Commun. **94**, 543 (1995).

[9] S. A. Crooker, J. J. Baumberg, F. Flack, N. Samarth, and D. D. Awschalom, Phys. Rev. Lett. **77**, 2814 (1996); Phys. Rev. B **56**, 7574 (1997).

[10] C. Buss, R. Pankoke, P. Leisching, J. Cibert, R. Frey, and C. Flytzanis, Phys. Rev. Lett. **78**, 4123 (1997).

[11] J. M. Kikkawa, I. P. Smorchkova, N. Samarth, and D. D. Awschalom, Science **277**, 1284 (1997).

[12] J. M. Kikkawa and D. D. Awschalom, Nature (London) **397**, 139 (1998).

[13] J. M. Kikkawa and D. D. Awschalom, Phys. Rev. Lett. **80**, 4313 (1998).

[14] H. Haug and A. P. Jauho, *Quantum Kinetics in Transport and Optics of Semiconductors* (Springer, Berlin, 1996).

[15] *Optical Orientation*, edited by F. Meier and B. P. Zachachrenya (North-Holland, Amsterdam, 1984).

[16] R. J. Elliott, Phys. Rev. **96**, 266 (1954).

[17] Y. Yafet, Phys. Rev. **85**, 478 (1952).

[18] G. L. Bir, A. G. Aronov, and G. E. Pikus, Zh. Éksp. Teor. Fiz. **69**, 1382 (1975) [Sov. Phys. JETP **42**, 705 (1975)]; G. E. Pikus and G. L. Bir, *ibid.* **60**, 195 (1971) [**33**, 108 (1971)].

[19] N. Linder and L. J. Sham, Physica E **2**, 412 (1998).

[20] Q. T. Vu, L. Bànyai, H. Haug, F. X. Camescasse, J. P. Likforman, and A. Alexandrou, Phys. Rev. B **59**, 2760 (1999).

[21] It is noted that the origin of the EHSE Hamiltonian proposed here is different from that by Bir *et al.* (Ref. 18). The origin here is the relativistic expansion of the Coulomb interaction between two electrons in the CB and hh VB respectively [see, e.g., V. B. Berestetskii, E. M. Lifshitz, and L.P. Pitaevskii, *Landau and*

Lifshitz Course of Theoretical Physics Vol. 4: Quantum Electrodynamics (Pergamon Press, Oxford, UK, 1989), Sec. 83]. Here, we do not need any band mixing due to the spin-orbit coupling, which is very small and there is no overlap integral of wavefunctions between CB and VB, which is required in the model by Bir *et al.* However, we are unable to rule out the mechanism proposed by Bir *et al.* without a first principle band structure calculation. In this paper, we only use a phenomenological parameter to describe the matrix element. It is therefore noted that under such an approximation, both mechanisms proposed here and that by Bir *et al.* can be described by the same kinetics presented in this paper. A first principle investigation is necessary in determining which one is dominant.

[22] This many body interaction Hamiltonian can be derived from the interaction potential $e^2/\epsilon_0 r|_{r=|\mathbf{r}_1-\mathbf{r}_2|}+e^2/4\epsilon_0 m_e m_h[1/r^3-3z^2/r^5-(8\pi/3)\delta(r)]|_{r=|\mathbf{r}_1-\mathbf{r}_2|}J_z S_z$. The first term describes the Coulomb potential between two electrons. One can use a plane-wave approximation to get the first term in Eq. (3). The second term is the EHSE (Ref. 21) with J representing the spin of the electron in the hh VB and S denoting the spin of the electron in the CB. For the 2D case, a plane-wave approximation cannot be applied to this term and one has to use the wave function of the material to calculate the matrix elements U_q and U'_q for the second and third terms in Eq. (3).

[23] It is noted that it is also true that the contribution from EHSE to the spin-coherence scattering term is also much smaller than that from Coulomb scattering. However the fact that $\Sigma_k \partial\rho_{cc,k,\sigma-\sigma}/\partial t|_{\text{scat}}^{\text{EHSE}} \neq 0$ makes it contribute to the long time decay of the spin coherence whereas the fact that $\Sigma_k \partial f_{\nu,k,\sigma}/\partial t|_{\text{scat}}^{\text{EHSE}}=0$ makes its contribution to the scattering of electron (hole) distribution negligible. Its contribution to the scattering of optical coherence is obviously negligible as the later vanishes within the first few picoseconds.

[24] Th. Östreich, K. Schönhammer, and L. J. Sham, Phys. Rev. Lett. **74**, 4698 (1995).

[25] L. Bányai, E. Reitsamer, and H. Haug, J. Opt. Soc. Am. B **13**, 1278 (1996).

[26] M. Lindberg, R. Binder, and S. W. Koch, Phys. Rev. A **45**, 1865 (1996).

[27] J. M. Kikkawa (private communication).

[28] *Numerical Data and Functional Relationships in Science and Technology*, edited by K. H. Hellwege, O. Madelung, M. Schultz, and H. Weiss, Landolt-Börnstein, New Series, Vol. 17 (Springer-Verlag, Berlin, 1982).

[29] H. Haug and S. W. Koch, *Quantum Theory of the Optical and Electronic Properties of Semiconductors* (World Scientific, Singapore, 1993).

[30] T. Kuhn and F. Rossi, Phys. Rev. Lett. **69**, 977 (1992).

[31] X. Marie, T. Amand, P. Le Jeune, M. Pailard, P. Renucci, L. E. Golub, V. D. Dymnikov, and E. L. Ivchenko, Phys. Rev. B **60**, 5811 (1999).

[32] P. Boguslawski, Solid State Commun. **33**, 389 (1980).